Research Article

Assessment of Local Reaction to Vaccines in Live Piglets with Magnetic Resonance Imaging Compared to Histopathology

Maren Bernau [1], Prisca V. Kremer [1,2], Lena S. Kreuzer [1], Daniela Emrich [3], Elke Pappenberger [1], Klaus Cussler [4], Andreas Hoffmann [4], Miriam Leipig [3], Walter Hermanns [3] and Armin Manfred Scholz [1]

[1]Livestock Center Oberschleissheim, Veterinary Faculty of the Ludwig-Maximilians-University Munich, Oberschleissheim, Germany; [2]University of Applied Sciences Weihenstephan-Triesdorf, Weidenbach, Germany; [3]Institute of Veterinary Pathology, Centre for Clinical Veterinary Medicine, Ludwig-Maximilians-University Munich, Munich, Germany; [4]Paul-Ehrlich-Institut, Langen, Germany

Summary

The safety of veterinary vaccines is assessed in clinical trials in Europe. The assessment of the local tissue reaction to vaccination by magnetic resonance imaging (MRI) could reduce the number of animals needed because repeated examinations can be performed in the same animal over time. The present study compared the evaluation of local tissue reactions to vaccination using MRI in live pigs with histopathology of porcine tissue, the current gold standard in regulatory safety testing. Eight piglets each were administered one of two commercial vaccines into marked injection sites. All animals were sedated and scanned repeatedly by MRI using a contrast agent up to day 29 after vaccination. On day 29, the animals were euthanized and underwent a pathological examination. The MRI results were compared with the pathomorphological findings at the injection site by regression analysis. The MR images and the pathological examinations yielded matching results concerning the sizes of the affected tissue volumes or areas. The use of MRI for regulatory safety testing can reduce the number of animals needed to 8 per examination group. The volume of a local reaction and its progression over time can be evaluated and documented. If persistent lesions develop a final pathomorphological examination is needed to identify the kind and local distribution of the reaction.

Keywords: safety testing, magnetic resonance imaging, local reaction, pathomorphological examination, pig

1 Introduction

Local reactions are possible side effects of vaccination. These are mostly small and transient in the case of live viral vaccines but are often more pronounced in case of inactivated vaccines owing to the use of adjuvants. Adjuvant-induced local inflammatory reactions at the injection site are common but vary in extent depending on adjuvant type (Day, 2006; Patel and Heldens, 2009; Spickler and Roth, 2003).

Although veterinary vaccines undergo preclinical and clinical testing to ensure the safety of a product, the frequency and extent of side effects, like swelling, pain, granulomas or systemic effects such as fever or shock symptoms (Martinod, 1995; Roth, 1999) needs to be evaluated in field trials. These safety tests are mandated by the European Pharmacopoeia and other legal regulations for immunobiologicals (EC, 2001; EDQM, 2008). They demand a large number of animals, since all age categories of the target animal species for which the vaccine is intended must be tested and the local reaction has to be examined after vaccination including a pathomorphological examination of the vaccination site (EC, 2001; EDQM, 2008).

Imaging methods can be used to visualize tissue changes in the living proband. In human medicine magnetic resonance imaging (MRI) is an approved method for diagnosis and follow-

Received July 21, 2015;
Accepted October 5, 2015;
Epub November 5, 2015;
http://dx.doi.org/10.14573/altex.1507211

Tab. 1: Animal description, subdivided into the examination groups with the number of animals (n), gender, average weight at the first and last examination day and vaccine ingredients

group	n	gender	Ø weight (kg)		vaccine ingredients
			first day	last day	
I	8	4♂+4♀	12.5 ± 1.5	24.1 ± 3.7	Mycoplasma hyopneumoniae I, light mineral oil, aluminium (as hydroxide), thiomersal
II	8	4♂+4♀	10.1 ± 1.4	16.6 ± 3.6	Mycoplasma hyopneumoniae II, carbopol, thiomersal

up of musculoskeletal diseases (Kuo and Carrino, 2007; Messineo et al., 1998; Schedel et al., 1992; Walker, 2008; Young and Bydder, 2003). MRI has been used in mice to evaluate antigen clearance after vaccination (Brewer et al., 2014). Other studies reported the use of imaging technologies in pharmacological research (Rudin, 1994; Rudin et al., 1995). Concerning muscle tissue, various alterations resulting from trauma, infection, inflammation or edema can be detected using MRI (Lovitt et al., 2006; May et al., 2000; Schrank et al., 2005; Shellock et al., 1996; Pathria and Boutin, 2009) due to signal intensity changes, especially when performing different protocols (T1- and T2-weightenings; see Hodgson, 2010; Pipe, 1999). Local reactions can be detected via MRI (Brewer et al., 2014; Rudin, 1994; Rudin et al., 1995) and results of our own study in pigs (Bernau et al., 2015) showed that MRI allows the documentation of local reactions after vaccination in the live pig, scanned repeatedly over 29 days.

In this study, we repetitively evaluated the volumes of local reaction after vaccination with commercial veterinary vaccines via MRI over a maximum of 29 days in pigs. To verify the results, the animals were euthanized on the last day of MRI examination and underwent a histopathological examination of the injection site.

2 Animals and methods

2.1 Animals

For this study 16 German Landrace piglets were randomly divided into two experimental groups (n=8; Tab. 1). All animals were kept according to the German national animal welfare regulations (Germany, 2013; German Federal Ministry for Food, Agriculture and Consumer Protection, 2009; EU, 2010, Directive 2010/63/EU). The animal experiment was licensed by the District Government of Upper Bavaria (registry number: 55.2-1-54-2532-138-11). The animals were born and raised on a conventional pig farm. They were housed in groups. All boxes were enriched with balls and metal chains equipped with diverse chewable material to satisfy their natural behavior.

The pigs were marked using a circular tattoo needle (diameter 0.3 cm) on the left neck skin (vaccination side) three weeks before the animals reached the specified vaccination age. Two commercial vaccines were used, both with 2 ml injection volume. Each group of piglets was injected intramuscularly with one vaccine into the center of the tattoo circle when they were approximately 6 weeks old. The composition of the vaccines is shown in Table 1. All animals were healthy and had not been vaccinated prior to the experiment.

2.2 Magnetic Resonance Imaging (MRI)

MRI test procedure

For this study an open low-field MRI system (Siemens Magnetom Open; 0.2 Tesla magnetic field strength) was used to detect and evaluate the local reaction inside the neck region of the pigs. All pigs had to be anaesthetized for MR scanning to avoid movement and to guarantee an excellent image quality. Anesthesia was performed with a combination of azaperone (2 mg per kg body weight) and ketamine (10-15 mg per kg body weight) given intramuscularly (Germany, 2005). Anesthetics were injected into the hind leg muscles to avoid any interaction with vaccination-induced tissue changes at the neck. None of the animals received any injection into the neck musculature prior to experimental vaccination.

The piglets were vaccinated at day 0 and examined by MRI at days 1, 3, 8, 15, 22 and 29 after vaccination. Up to now, only the results of day 29, the scheduled end of the study, were used for comparison with the pathomorphological examination as described below.

Each animal underwent T1- and T2- weighted sequences with two directions of acquisition (coronal and axial), using the small body coil as receiver. The corresponding sequence parameters are shown in Table 2. All pigs were bedded in a prone position with front limbs flexed and hind limbs extended. Prone bedding is necessary to evaluate both neck sides simultaneously without creating artifacts due to the bedding. The vaccination point was positioned in the middle of the coil.

A Gadolinium-based contrast agent (Gadobutrol, Bayer Vital GmbH, Leverkusen; 0.3 mmol per kg body weight) was administered via intravenous injection in order to improve the detection of potential local reactions in the MR images. Gadobutrol is a nonionic macrocyclic extracellular MRI contrast agent with a high T1 relaxivity, which reduces the T1 relaxation time and therefore increases the signal intensity in T1-weighted MR images (Bayer Health Care, 2011; Vogler et al., 1995). Because Gadobutrol is not listed in the Annex of Directive EC 470/2009 (EC, 2009), its use is not permitted in animals intended for human consumption.

For MRI examination the following protocol was used:

1. T1-weighted spin echo sequence with coronal acquisition, native without contrast agent use ($T1_{cn}$)

2. Intravenous application of Gadobutrol (0.3 mmol per kg body weight)
3. T2-weighted spin echo sequence with the same coronal acquisition as $T1_{cn}$ ($T2_c$)
4. T1-weighted spin echo sequence with the same coronal acquisition as $T1_{cn}$, with contrast agent ($T1_{cCA}$)
5. T1-weighted spin echo sequence with axial acquisition, with contrast agent ($T1_{aCA}$)

(T1 = T1-weighted; T2 = T2-weighted; $_c$ = coronal acquisition; $_a$ = axial acquisition; $_n$ = native, without contrast agent; $_{CA}$ = with contrast agent)

MR image evaluation

For image evaluation the Able 3D Doctor® Software (Able Software Corp. Lexington, MA, USA. 2007: ASC 3DDR-BN#07032 (FDA approved)) was used, in order to measure the local reaction. The volumes of regions with increased signal intensity at the vaccination side (VS) and at the control side (CS) were bordered semiautomatically at defined signal intensities on a grey scale level from 0 (black) - 4096 (white) (Bernau et al., 2015). A region of interest (ROI) was created to cover the largest extent of the area with increased signal intensity at the VS. Inside this ROI, regions with grey values close to white (increased signal intensities) were classified as hyper-intense regions. Within the same image the ROI of the VS was mirrored to the CS. Regions inside CS with the same thresholds for signal intensity as on the VS were bordered as well. Five images from each sequence – starting at the injection point – were evaluated in ventral direction accordingly to create volumes of interest.

2.3 Pathomorphological examination

On day 29 after vaccination, the animals were euthanized in narcosis by an intracardial injection of sodium pentobarbital (Euthadorm®, CP-Pharma; 80 mg per kg body weight).

A whole body necropsy was performed to evaluate the health status of the animal. Furthermore, the whole neck region was examined and sampled. Tissue up to the level of the spine was removed and underwent fixation in 4%-formaldehyde solution for two days. After this time, neck regions were sliced transversally, in about 1 cm thick slices, from both sides up to a distance of one centimeter to the application site. Every slice was carefully evaluated for the presence of pathological changes including discolorations, heterogeneity of tissue architecture, fluid accumulations or foreign structures and compared to the contralateral side. Any pathological change was noted and its dimension was measured at the level of the widest extent on a cutting surface by ruler.

The remaining slice of 2 cm thickness was trimmed from laterally up to a distance of 1 cm to the injection site. The remaining tissue block was horizontally cut into slices of 3 mm thickness and numbered, beginning at the level of the skin (Fig. 1). Every slice was postfixed for a further 24 h in 4%-formaldehyde solution. Afterwards, the slices underwent paraffin embedding or glycol-methacrylate-methylmethacrylate (GMA-MMA) embedding in an alternate manner, beginning with the skin by paraffin embedding.

Standard staining procedures (H&E and Giemsa) were performed in every level of both paraffin and GMA-MMA samples. Histopathological examination was performed by two independent pathologists. Any lesion was noted and the extent of inflammation was estimated in percentage (%) of each slide. First, max_extent (%) was calculated as mean of the slides with maximum extent of inflammation per group. Second, av_extent (%) was calculated as mean of all slides showing inflammation per group.

2.4 Statistical analysis

For the statistical analysis, the average MRI volume difference (Vol_diff) between VS and CS (including the standard error) was calculated for each sequence and tested against zero by

Tab. 2: MRI parameters used for the examination, subdivided into the T1-weighted (T1) and the T2-weighted (T2) sequence

MRI parameter	T1		T2
	coronary	axial	coronary
TR (ms)	814	814	5690
TE (ms)	17	17	102
pixel size	1.30 x 0.70	1.56 x 0.76	1.43 x 0.78
FOV (mm)	180	200	200
matrix	54%; 138 x 256	50%; 128 x 256	55%, 140 x 256
number of slices	22	22	22
slice thickness (mm)	4	4	4
distance factor	0.5	0.5	0.5
examination time	5 min 40 sec	5 min 15 sec	5 min 48 sec

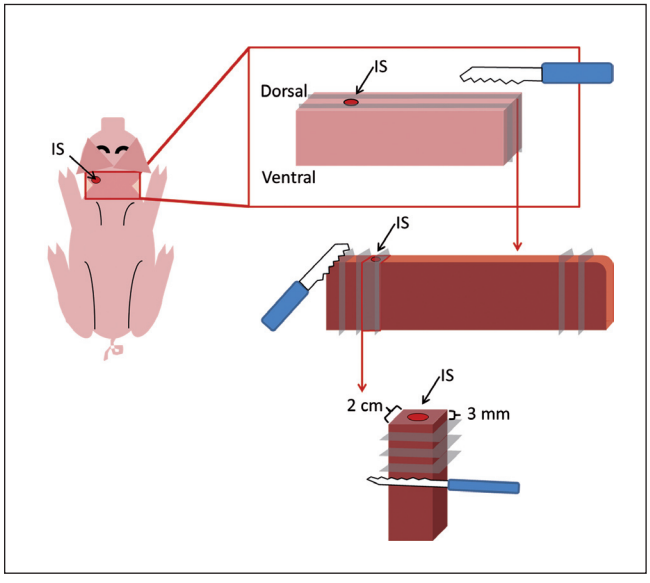

Fig. 1: Schematic description of the procedure of tissue trimming (IS = injection site)

t-test using SAS 9.3 software (SAS Software 9.3. Institute Inc., Cary, North Carolina, USA, 2010), (Tab. 3). This t-test was also performed for the pathological variables (av_extent and max_extent; Tab. 3).

In addition, a single regression analysis was performed using the individual MRI variables Vol_diff for each sequence and the individual pathological variables max_extent and av_extent (Tab. 4).

The significance level was set to p = 0.05 in both cases. Finally, an unpaired t-test was applied for the comparison of the two vaccines, both for the MRI and the pathological data.

3 Results

Data of the MRI examination and the pathomorphological examination (as av_extent and max_extent) both representing day 29 after vaccination are displayed in Table 3 and are represented as one MR image per group and the corresponding histopathological images (overview and close up) in Figure 2.

The coronal and axial T1-weighted sequences of group II taken after application of the contrast agent ($T1_{cCA}$ and $T1_{aCA}$) showed greater volume differences than in group I that were statistically significant for $T1_{aCA}$ (p = 0.02). This finding corresponded with the results of the pathomorphological examination, where group II showed a significantly larger average or maximum extent of inflammation compared to group I.

Pathomorphological examination confirmed that none of the animals suffered from a disease process interfering with the aim of the study. On the last examination day, none of the animals showed any macroscopically visible alteration at the surface of the neck tissue. Only one of the piglets in group II showed a mild discoloration of muscle tissue with a diameter of 4 mm at the injection site. Microscopically, each vaccination resulted in a lesion of variable degree in all pigs of both groups. In detail, histological examination revealed granulomatous inflammation and the presence of foreign material at the injection sites of both groups.

The results of the regression analysis are shown in Table 4 and Figure 3. Low to high regression coefficients (R^2 = 0.05 - 0.56) were achieved for the relationship between MRI and pathomorphological data. Significant results (p < 0.05) were achieved when contrast agent was used during MR imaging ($T1_{cCA}$_Vol_diff; $T1_{aCA}$_Vol_diff). The av_extent compared with the $T2_c$_Vol_diff showed also a significant relationship (p = 0.0047). The error term (root mean square error, RMSE) was largest, however,

Tab. 3: Mean volume differences for all used MRI sequences at day 29 after vaccination and means of the pathomorphological examinations

Group	$T1_{cn}$ Vol_diff ± SE (cm^3)	$T1_{cCA}$ Vol_diff ± SE (cm^3)	$T2_c$ Vol_diff ± SE (cm^3)	$T1_{aCA}$ Vol_diff ± SE (cm^3)	Pathological examination	
					av_extent ± SE (%)	max_extent ± SE (%)
I	0.03 ± 0.03	0.09 ± 0.04 (p = 0.08)	0.14 ± 0.29	-0.04 ± 0.04 (p = 0.30)	11.54 ± 1.57	16.75 ± 4.06 (p = 0.004)
II	0.05 ± 0.08	0.37 ± 0.14 (p = 0.03)	1.55 ± 0.72 (p = 0.07)	0.19 ± 0.08 (p = 0.05)	21.08 ± 2.60	31.25 ± 3.24
I vs. II	p = 0.8	p = 0.08	p = 0.09	p = 0.02	p = 0.007	p = 0.01

$T1_{cn}$ = T1-weighted coronal sequence, native without contrast agent. $T1_{cCA}$ = T1-weighted coronal sequence, with contrast agent. $T2_c$ = T2-weighted coronal sequence. $T1_{aCA}$ = axial T1-weighted sequence, with contrast agent. *Vol_diff* describes the difference for the volume of interest from VS minus CS. All average volume differences are specified with the corresponding standard error (SE). av_extent = % of extent of local reaction in all affected slices; max_extent = % of maximum extent in one slice. P-values in parenthesis. The extents from pathological examination were all significantly different from zero (p = 0.05).

Tab. 4: Results of the regression analysis (significance level p-value < 0.05), with regression coefficient (R^2), RMSE (cm^3) and the corresponding p-value

Variable	av_extent			max_extent		
	R^2	RMSE (cm^3)	p-value	R^2	RMSE (cm^3)	p-value
$T1_{cn}$_Vol_diff	0.10	0.16	0.2269	0.05	0.17	0.4184
$T1_{cCA}$_Vol_diff	**0.55**	0.22	**0.0010**	**0.56**	0.22	**0.0009**
$T2_c$_Vol_diff	**0.45**	1.28	**0.0047**	0.24	1.50	0.0542
$T1_{aCA}$_Vol_diff	**0.52**	0.15	**0.0016**	**0.41**	0.17	**0.0079**

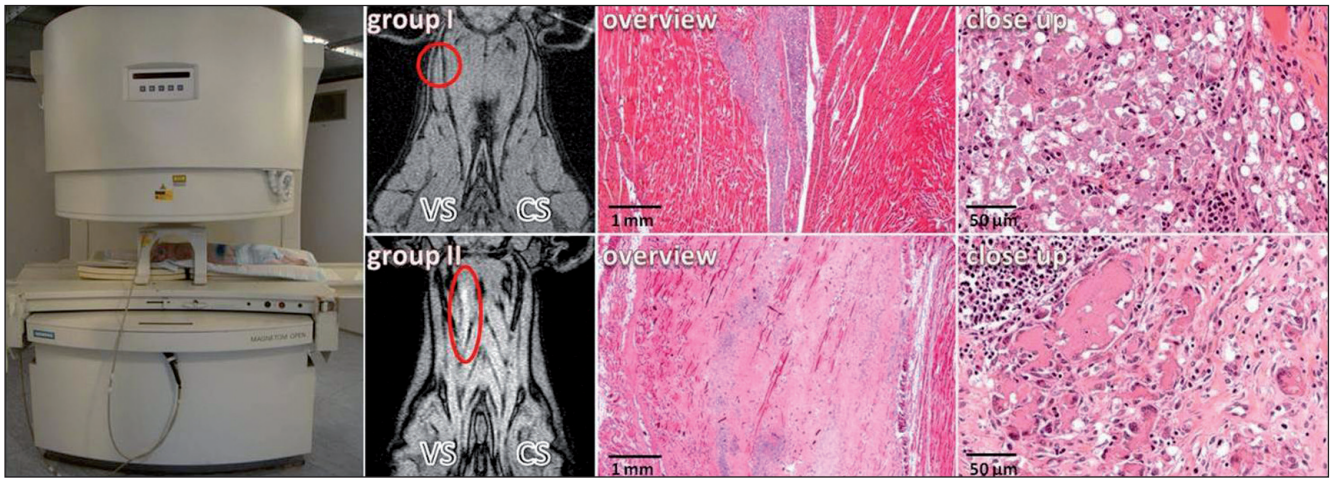

Fig. 2: MRI examination of a piglet, lying on the belly with front limbs flexed and hind limbs extended
MR image of a piglet of group I (upper line) and of a piglet of group II (lower line) with the corresponding histopathologic image (overview and close up) of this animal of each group.
Group I: MRI: Small signal intensity increase at VS. Overview: focal extensive fibrosis and hypercellularity of the skeletal musculature. Close up: granulomatous inflammation with cytoplasmatic granular, slightly basophilic foreign material in macrophages next to nests of lymphocytes and plasma cells.
Group II: MRI: Extended signal intensity increase at VS. Overview: focal extensive fibrosis and scarring of skeletal musculature and multifocal hypercellularity. Close up: granulomatous inflammation with presence of multinucleated giant cells and accumulation of homogeneous, azidophilic cytoplasmatic foreign material in macrophages next to nests of lymphocytes and plasma cells embedded in fibrous tissue.

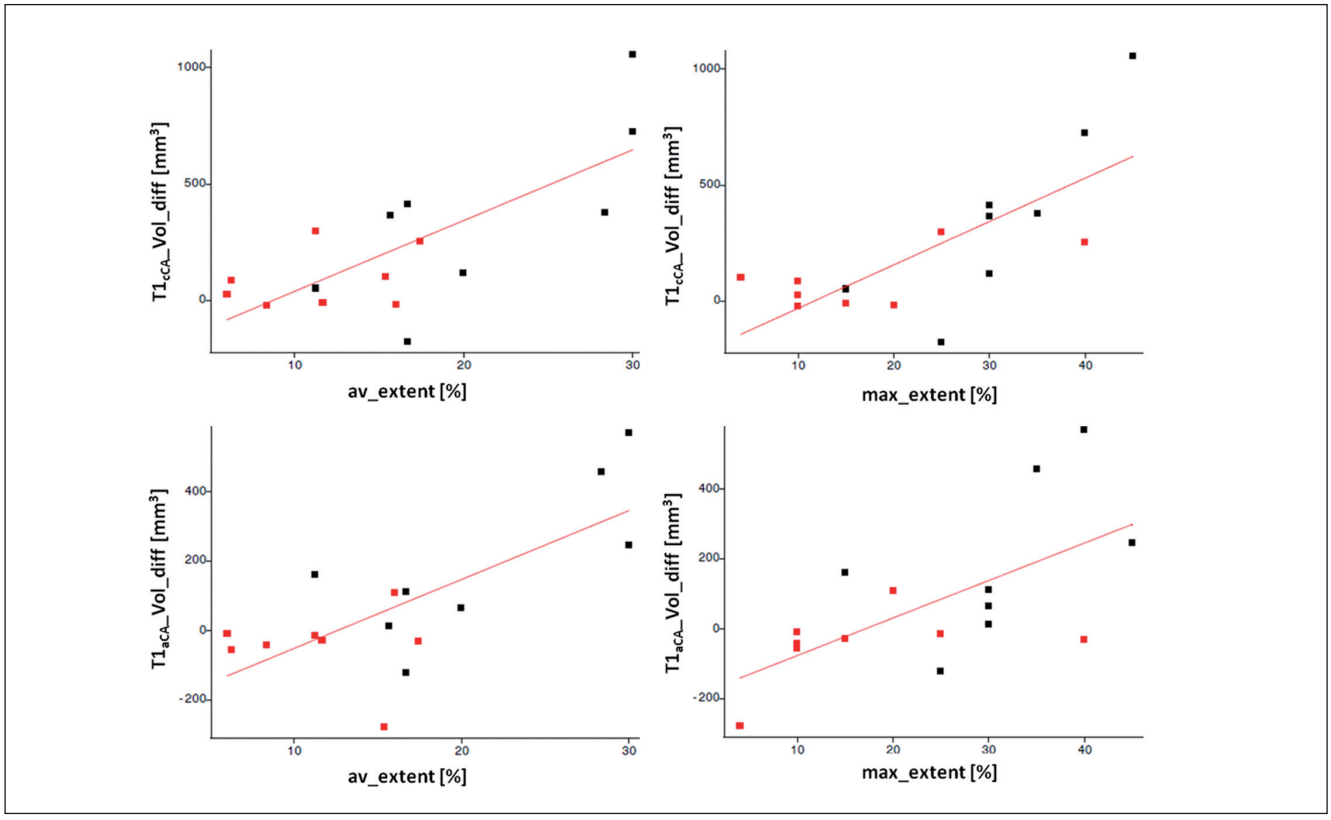

Fig. 3: Graphs of the regression analysis of the contrast agent MRI volume differences ($T1_{cCA}$, $T1_{aCA}$ each in mm³) and the pathomorphological data (av_extent, max_extent each in %)
Group I as red squares and group II as black squares

for the relationship between the T2-weighted sequences and the pathomorphological data (1.28 and 1.5 cm^3). RMSE was comparably lower for the T1-weighted sequences (0.15 - 0.22 cm^3).

Figure 3 shows the distribution of the data, with group I as red squares and group II as black squares. Both imaging directions (axial or coronal T1-weighted sequence after application of contrast agent) revealed the same tendency for both groups resulting in a tendency in animals of group II towards larger Vol_diff (MRI) and a larger histopathologically defined extent of inflammation than in animals of group I.

4 Discussion

Injectable medicines for veterinary applications must be checked for local and systemic adverse effects during the development and licensing process. The reactogenicity especially of adjuvanted vaccines at the injection site is of major importance because of animal welfare concerns. In target animal species intended for human consumption long-lasting local reactions may affect meat quality. In principle, every vaccine exhibits a different extent of local reaction at the vaccination site mainly due to the interaction of the adjuvant(s) and the antigens (Spickler and Roth, 2003).

Vaccinations performed in the present study caused a detectable local reaction within the neck tissue of the pigs in both groups that was visible in MR images and confirmed by pathomorphological examination (Fig. 2).

For both methods, the detected local reactions varied regarding their extent (Tab. 3, Fig. 2, 3). Both methods detected a higher Vol_diff (MRI; in all sequences) as well as a higher av_extent and max_extent (pathological examination; Tab. 3, Fig. 3) in group II on the last examination day.

The use of the contrast agent Gadobutrol led to statistically significant results in group II, both for the coronary and axial T1-weighted sequences (Tab. 4, Fig. 3). Gadobutrol reduces T1 relaxation time and increases the signal intensity in T1-weighted MR images (Vogler et al., 1995). Here, the contrast agent highlighted small local reactions by semiautomatic image evaluation as confirmed by regression analysis (Tab. 4, Fig. 3).

Using multiple MR sequences, diverse pathologic alterations can be detected (Berquist et al., 1985). Pathologic conditions like hematoma, edema, fatty infiltration or inflammation result in hyper-intense signal alterations (visible as very bright voxels) in tissue parameters by different image weightings (Lovitt et al., 2006; May et al., 2000; Schrank et al., 2005). For this study, T1- and T2-weighted image sequences were used (Tab. 2) and the image evaluation was performed by a semiautomatic bordering of hyper-intense signals at the VS and CS, in order to create volumes (see Vol_diff, Tab. 3). These created volumes describe local tissue reactions.

Regions with hyper-intense signals in T2-weighted MR images represent an increase in fat or water (Lovitt et al., 2006; May et al., 2000) and additionally, inflammation or increased blood flow in the early stage of a myopathic condition (Schrank et al., 2005). In the present study all hyper-intense regions inside VS – which were not detected in CS – were interpreted as an increase of interstitial water (edema), since pathologic fatty infiltration only results from muscle necrosis in chronic muscle disorders or denervation atrophy (Schrank et al., 2005). Unfortunately, these mild edematous residues were not detectable microscopically in this study. Trimming lesions of the tissue could have obscured mild edematous tissue distensions, especially when these were located at tissue interfaces.

Regions with hyper-intense signals in T1-weighted MR images can represent inflamed tissue, fatty infiltration or hematoma (May et al., 2000; Schrank et al., 2005). In the present study, pathomorphological examination confirmed an inflammatory process at the injection site in all animals. Since all other injections were given into the ham muscle, the detected alterations in the neck region can be solely related to the vaccination. Therefore, all regions with hyper-intense signal in T1-weighted images were attributed to local reactogenicity.

The detected MRI volume differences varied depending on the vaccine used (Tab. 3). These variations could be due to the adjuvants of the vaccines, which are known to determine the extent and duration of the local reaction (Batista-Duharte et al., 2013; Edelman, 1980; Gupta et al., 1993).

The pathomorphological examination confirmed a degree of local reaction that related to the MRI data (Tab. 4, Fig. 3) independently of the vaccine used. Nevertheless some factors influence the interpretation of both methods: first, MRI provides numerical values after image evaluation, whereas the volume of a lesion cannot be as easily ascertained histopathologically. Second, local reactions of small dimension could be undervalued in MR images, since the spatial resolution could be reduced due to a large voxel size.

Both methods have advantages and limitations regarding the evaluation of local reactogenicity. For MRI, the user defines the image contrast that is used to border the local reaction semi-automatically. A fully automated image analysis would be more objective and could secure inter-observer reliability. Nevertheless, using MRI offers a three-dimensional imaging tool and allows the evaluation of the whole neck region. Furthermore, it can be performed repetitively on the live animal. Pathomorphological examination, on the other hand, represents only a segment of the whole neck tissue. The pathomorphological evaluation of the whole neck region is costly and time consuming and cannot be performed in routine safety testing. Therefore, it is imperative that the injection site is permanently marked over the whole examination period until pathomorphological examination is performed. The kind of cellular infiltration, tissue destruction and deposition of foreign materials can be examined microscopically. In addition, special staining methods and immunohistochemical analysis can help to analyze and interpret local reactions in more detail.

5 Conclusion

Non-invasive MRI allows evaluation of the local reaction repeatedly in the same animal over the course of a clinical trial.

The MRI data are in line with the results of the pathomorphological evaluation as illustrated in this study by examining two different commercial vaccines. In our study the use of a low field MRI system, a minimum number of 8 animals per group with permanently marked injection sites, and the use of contrast agent to visualize poorly demarcated or multifocally distributed minor tissue lesions provide an appropriate method to achieve results comparable to the gold standard, i.e., the pathomorphological examination. This approach allows reduction of the number of animals needed for preclinical and clinical research studies in the development of biologicals. To evaluate the character and details of local reactions, pathomorphological examination may still be necessary if tissue lesions are still present, but could likely be reduced to a lesser number of time points and, therefore, animals. To establish the MRI method, it is initially advisable to conduct both methods in parallel for each examination day and for numerous vaccine preparation to gain experience for every animal species and category.

References

Batista-Duharte, A., Portuondo, D., Carlos, I. Z. and Pérez, O. (2013). An approach to local immunotoxicity induced by adjuvanted vaccines. *Int Immunopharmacol 17*, 526-536. http://dx.doi.org/10.1016/j.intimp.2013.07.025

Bayer Health Care (2011). Bayer product brochure "*Höchstkonzentriert auf den Kontrast*" Gadovist 1.0, 5th edition.

Bernau, M., Kremer, P. V., Pappenberger, E. et al. (2015). Safety testing of veterinary vaccines using magnetic resonance imaging in pigs. *ALTEX 32*, 51-58. http://dx.doi.org/10.14573/altex.1407071

Berquist, T. H., Brown, M. L., Fitzgerald, R. H. and May, G. R. (1985). Magnetic resonance imaging: Application in musculoskeletal infection. *Magn Reson Imaging 3*, 219-230. http://dx.doi.org/10.1016/0730-725X(85)90350-9

Brewer, K. D., Lake, K., Pelot, N. et al. (2014). Clearance of depot vaccine SPIO-labeled antigen and substrate visualized using MRI. *Vaccine 32*, 6956-6962. http://dx.doi.org/10.1016/j.vaccine.2014.10.058

Day, M. J. (2006). Vaccine side effects: Fact and fiction. *Vet Microbiol 117*, 51-58. http://dx.doi.org/10.1016/j.vetmic.2006.04.017

EC – European Commission (2001). Directive 2001/82/EC of the European Parliament and of the Council of 6 November 2001 on the Community code relating to veterinary medicinal products. Annex I: Requirements and analytical protocol, safety tests, pre-clinical and clinical for tests of veterinary medicinal products. Title II: Requirements for immunological veterinary medicinal products. Part 7: Safety testing.

EC (2009). Regulation (EC) of No 470/2009 of the European Parliament and the Council of 6 May 2009 laying down Community procedures for the establishment of residue limits of pharmacologically active substances in foodstuffs of animal origin, repealing Council Regulation (EEC) No 2377/90 and amending Directive 2001/82/EC of the European Parliament and of the Council and Regulation (EC) No 726/2004 of the European Parliament and of the Council.

EDQM – European Directorate for the Quality of Medicines and Health Care (2008). *European Pharmacopoeia (Ph. Eur.)*. 6th edition. Volume 1, Chapter 5.2.6. Evaluation of safety of veterinary vaccines and immunosera (p 536 ff.).

EU – European Union (2010). Directive 2010/63/EU of the European Parliament and of the Council of 22 September 2010 on the protection of animals used for scientific purposes. *Off J Eur Union L276*, 33-79. http://eur-lex.europa.eu/LexUriServ/LexUriServ.do?uri=OJ:L:2010:276:0033:0079:en:PDF

Edelman, R. (1980). Vaccine adjuvants. *Rev Infect Dis 2*, 370-383. http://dx.doi.org/10.1093/clinids/2.3.370

German Federal Ministry for Food, Agriculture and Consumer Protection (2009). Verordnung zum Schutz landwirtschaftlicher Nutztiere und anderer zur Erzeugung tierischer Produkte gehaltener Tiere bei ihrer Haltung (TierSchNutztV) in der Fassung der Bekanntmachung vom 22. August 2006 (BGBl. I S. 2043), die durch Artikel 1 der Verordnung vom 1. Oktober 2009 (BGBl. I S. 3223) geändert worden ist. Neugefasst durch Bek. v. 22.8.2006 I 2043; geändert durch Art. 1 V v. 1.10.2009 I 3223. http://www.gesetze-im-internet.de/tierschnutztv/index.html

Germany (2005). Medicinal Products Act in the version published on 12 December 2005 (Federal Law Gazette [BGBl.]) Part I p. 3394, last amended by Article 1 of the Law of 19th October 2012 (Federal Law Gazette I p. 2192). http://www.gesetze-im-internet.de/englisch_amg/medicinal_products_act.pdf

Germany (2013). Tierschutzgesetz in der Fassung der Bekanntmachung vom 18. Mai 2006 (BGBl. I S. 1206, 1313), das durch Artikel 4 Absatz 90 des Gesetzes vom 7. August 2013 (BGBl. I S. 3154) geändert worden ist. Neugefasst durch Bek. v. 18.5.2006 I 1206, 1313; zuletzt geändert durch Art. 1 G v. 4.7.2013 I 2182 (Animal Protection Law). http://www.gesetze-im-internet.de/tierschg/

Gupta, R. K., Relyveld, E. H., Lindblad, E. B. et al. (1993). Adjuvants – a balance between toxicity and adjuvanticity. *Vaccine 11*, 293-306. http://dx.doi.org/10.1016/0264-410X(93)90190-9

Hodgson, R. J. (2010). The basic science of MRI. *Orthop Trauma 25*, 119-130. http://dx.doi.org/10.1016/j.mporth.2010.12.002

Kuo, G. P. and Carrino, J. A. (2007). Skeletal muscle imaging and inflammatory myopathies. *Curr Opin Rheumatol 19*, 530-535. http://dx.doi.org/10.1097/BOR.0b013e3282efdc66

Lovitt, S., Moore, S. L. and Marden, F. A. (2006). The use of MRI in the evaluation of myopathy. *Clin Neurophysiol 117*, 486-495. http://dx.doi.org/10.1016/j.clinph.2005.10.010

Martinod, S. (1995). Risk assessment related to veterinary biological: side-effects in target animals. *Rev Sci Tech Off Int Epiz 14*, 979-989.

May, D. A., Disler, D. G., Jones, E. A. et al. (2000). Abnormal signal intensity in skeletal muscle at MR imaging: Patterns, pearls, and pitfalls. *Radiographics 20*, 295-315. http://dx.doi.org/10.1148/radiographics.20.suppl_1.g00oc18s295

Messineo, D., Cremona, A., Trinci, M. et al. (1998). MRI in the study of distal primary myopathopies and of muscular al-

terations due to peripheral neuropathies: possible diagnostic capacities of MR equipment with low intensity field (0.2 T) dedicated to peripheral limbs. *Magn Reson Imaging 16*, 731-741. http://dx.doi.org/10.1016/S0730-725X(98)00080-0

Patel, J. R. and Heldens, J. G. M. (2009). Immunoprophylaxis against important virus diseases of horses, farm animals and birds. *Vaccine 27*, 1797-1810. http://dx.doi.org/10.1016/j.vaccine.2008.12.063

Pathria, M. N. and Boutin, R. D. (2009). Magnetic resonance imaging of muscle. In J. Hodler, G. K. von Schulthess and C. L. Zollikofer (eds.), *Musculoskeletal Diseases 2009-2012* (57-62). Springer Verlag. http://dx.doi.org/10.1007/978-88-470-1378-0_10

Pipe, J. G. (1999). Basic spin physics. *Magn Reson Imaging Clin N Am 7*, 607-627.

Roth, J. A. (1999). Mechanistic bases of adverse vaccine reactions and vaccine failures. *Adv Vet Med 41*, 681-700. http://dx.doi.org/10.1016/S0065-3519(99)80053-6

Rudin, M. (1994). In vivo magnetic resonance imaging and spectroscopy in pharmacological research: Applications to drug development and profiling. *Eur J Pharm Sci 2*, 50-52. http://dx.doi.org/10.1016/0928-0987(94)90066-3

Rudin, M., Beckmann, N., Mir, A. and Sauter, A. (1995). In vivo magnetic resonance imaging and spectroscopy in pharmacological research: Assessment of morphological, physiological and metabolic effects of drugs. *Eur J Pharm Sci 3*, 255-264. http://dx.doi.org/10.1016/0928-0987(95)00012-3

Schedel, H., Reimers, C. D., Nägele, M. et al. (1992). Imaging techniques in myotonic dystrophy. A comparative study of ultrasound, computed tomography and magnetic resonance imaging of skeletal muscles. *Eur J Radiol 15*, 230-238. http://dx.doi.org/10.1016/0720-048X(92)90113-N

Schrank, B., Urban, P. and Lörcher, U. (2005). Der Einsatz der Magnetresonanztomographie der Muskulatur bei der Diagnose neuromuskulärer Erkrankungen (Application of magnetic resonance imaging in the diagnosis of neuromuscular disease). *Klin Neuroradiol 15*, 241-255. http://dx.doi.org/10.1007/s00062-005-6419-1

Shellock, F. G., Tyson, L. L. and Fleckenstein, J. L. (1996). Diagnostic imaging of skeletal muscle exercise physiology and pathophysiology. In J. L. Fleckenstein, J. V. Crues and C. D. Reimers (eds.), *Muscle Imaging in Health and Disease* (113-132). Springer Verlag. http://dx.doi.org/10.1007/978-1-4612-2314-6_7

Spickler, A. R. and Roth, J. A. (2003). Adjuvants in veterinary vaccines: Modes of action and adverse effects. *J Vet Intern Med 17*, 273-281. http://dx.doi.org/10.1111/j.1939-1676.2003.tb02448.x

Vogler, H., Platzek, J., Schuhmann-Giampieri, G. et al. (1995). Pre-clinical evaluation of gadobutrol: A new, neutral, extracellular contrast agent for magnetic resonance imaging. *Eur J Radiol 21*, 1-10. http://dx.doi.org/10.1016/0720-048X(95)00679-K

Walker, U. A. (2008). Imaging tools for the clinical assessment of idiopathic inflammatory myositis. *Curr Opin Rheumatol 20*, 656-661. http://dx.doi.org/10.1097/BOR.0b013e3283118711

Young, I. R. and Bydder, G. M. (2003). Magnetic resonance: New approaches to imaging of the musculoskeletal system. *Physiol Meas 24*, R1-23. http://dx.doi.org/10.1088/0967-3334/24/4/R01

Conflicts of interest

The authors declare that they have no conflicts of interest.

Acknowledgements

This research was funded in total by the German Federal Ministry of Education and Research (BMBF project number 0316009B). Additionally, the authors thank Bayer Healthcare Deutschland and especially Miss Petra Theessen for their support in conducting the MRI sequences and concerning the use of contrast agent.

Correspondence to

Maren Bernau, Dr. med. vet.
Livestock Center Oberschleissheim
Veterinary Faculty Ludwig-Maximilians-University Munich
St. Hubertusstrasse 12
85764 Oberschleissheim
Germany
Phone: +49 89 2180 76061
e-mail: Maren.Bernau@lmu.de